

# Inverse Folding of RNA Pseudoknot Structures

James Z.M. Gao<sup>1</sup>, Linda Y.M. Li<sup>1</sup> and Christian M. Reidys<sup>1\*</sup>

<sup>1</sup> Center for Combinatorics, LPMC-TJKLC, Nankai University, Tianjin 300071, PR China

Email: Gao: gzm55@cfc.nankai.edu.cn; Li: liyanmei@mail.nankai.edu.cn; \*Reidys: duck@santafe.edu;

\*Corresponding author

## Abstract

---

**Background:** RNA exhibits a variety of structural configurations. Here we consider a structure to be tantamount to the noncrossing Watson-Crick and **G-U**-base pairings (secondary structure) and additional cross-serial base pairs. These interactions are called pseudoknots and are observed across the whole spectrum of RNA functionalities. In the context of studying natural RNA structures, searching for new ribozymes and designing artificial RNA, it is of interest to find RNA sequences folding into a specific structure and to analyze their induced neutral networks. Since the established inverse folding algorithms, `RNAinverse`, `RNA-SSD` as well as `INFO-RNA` are limited to RNA secondary structures, we present in this paper the inverse folding algorithm `Inv` which can deal with 3-noncrossing, canonical pseudoknot structures.

**Results:** In this paper we present the inverse folding algorithm `Inv`. We give a detailed analysis of `Inv`, including pseudocodes. We show that `Inv` allows to design in particular 3-noncrossing nonplanar RNA pseudoknot 3-noncrossing RNA structures—a class which is difficult to construct via dynamic programming routines. `Inv` is freely available at <http://www.combinatorics.cn/cbpc/inv.html>.

**Conclusions:** The algorithm `Inv` extends inverse folding capabilities to RNA pseudoknot structures. In comparison with `RNAinverse` it uses new ideas, for instance by considering sets of competing structures. As a result, `Inv` is not only able to find novel sequences even for RNA secondary structures, it does so in the context of competing structures that potentially exhibit cross-serial interactions.

---

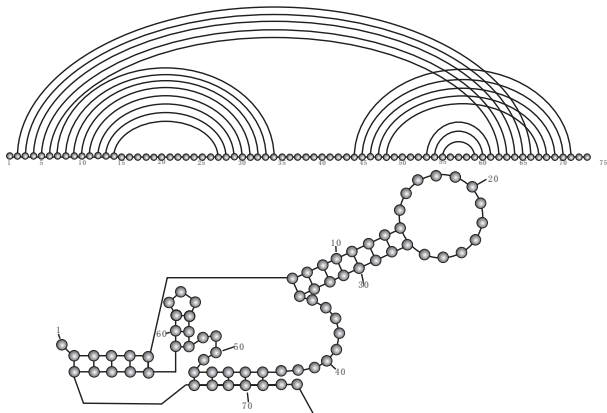


Figure 1: The pseudoknot structure of the glmS ribozyme pseudoknot P1.1 [7] as a diagram (top) and as a planar graph (bottom).

## 1 Introduction

Pseudoknots are structural elements of central importance in RNA structures [1], see Figure 1. They represent cross-serial base pairing interactions between RNA nucleotides that are functionally important in tRNAs, RNaseP [2], telomerase RNA [3], and ribosomal RNAs [4]. Pseudoknot structures are being observed in the mimicry of tRNA structures in plant virus RNAs as well as the binding to the HIV-1 reverse transcriptase in *in vitro* selection experiments [5]. Furthermore basic mechanisms, like ribosomal frame shifting, involve pseudoknots [6].

Despite them playing a key role in a variety of contexts, pseudoknots are excluded from large-scale computational studies. Although the problem has attracted considerable attention in the last decade, pseudoknots are considered a somewhat “exotic” structural concept. For all we know [8], the *ab initio* prediction of general RNA pseudoknot structures is NP-complete and algorithmic difficulties of pseu-

doknot folding are confounded by the fact that the thermodynamics of pseudoknots is far from being well understood.

As for the folding of RNA secondary structures, Waterman *et al* [9, 10], Zuker *et al* [11] and Nussinov [12] established the dynamic programming (DP) folding routines. The first mfe-folding algorithm for RNA secondary structures, however, dates back to the 60’s [13–15]. For restricted classes of pseudoknots, several algorithms have been designed: Rivas and Eddy [16], Dirks and Pierce [17], Reeder and Giegerich [18] and Ren *et al* [19]. Recently, a novel *ab initio* folding algorithm **Cross** has been introduced [20]. **Cross** generates minimum free energy (mfe), 3-noncrossing, 3-canonical RNA structures, i.e. structures that do not contain three or more mutually crossing arcs and in which each stack, i.e. sequence of parallel arcs, see eq. (1), has size greater or equal than three. In particular, in a 3-canonical structure there are no isolated arcs, see Figure 2.

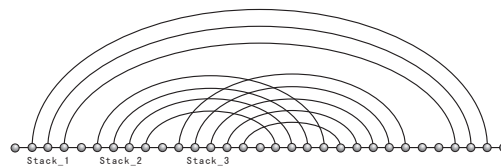


Figure 2:  $\sigma$ -canonical RNA structures: each stack of “parallel” arcs has to have minimum size  $\sigma$ . Here we display a 3-canonical structure.

The notion of mfe-structure is based on a specific concept of pseudoknot loops and respective loop-based energy parameters. This thermodynamic model was conceived by Tinoco and refined by

Freier, Turner, Ninio, and others [14, 21–25].

### 1.1 $k$ -noncrossing, $\sigma$ -canonical RNA pseudoknot structures

Let us turn back the clock: three decades ago Waterman *et al.* [26], Nussinov *et al.* [12] and Kleitman *et al.* in [27] analyzed RNA secondary structures. Secondary structures are coarse grained RNA contact structures, see Figure 3.

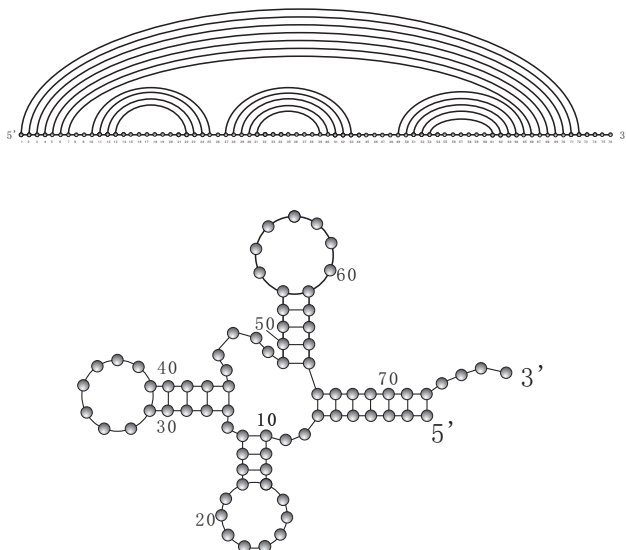


Figure 3: The phenylalanine tRNA secondary structure represented as 2-noncrossing diagram (top) and as planar graph (bottom).

Secondary structures can be represented as diagrams, i.e. labeled graphs over the vertex set  $[n] = \{1, \dots, n\}$  with vertex degrees  $\leq 1$ , represented by drawing its vertices on a horizontal line and its arcs  $(i, j)$  ( $i < j$ ), in the upper half-plane, see Figure 1 and Figure 4.

Here, vertices and arcs correspond to the nucleotides **A**, **G**, **U**, **C** and Watson-Crick (**A-U**, **G-C**) and (**U-G**) base pairs, respectively.

In a diagram, two arcs  $(i_1, j_1)$  and  $(i_2, j_2)$  are called crossing if  $i_1 < i_2 < j_1 < j_2$  holds. Accordingly, a  $k$ -crossing is a sequence of arcs  $(i_1, j_1), \dots, (i_k, j_k)$  such that  $i_1 < i_2 < \dots < i_k < j_1 < j_2 < \dots < j_k$ , see Figure 5.

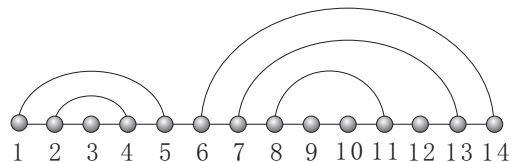


Figure 4: Setting  $k = 2$  we observe that secondary structures are a particular type of  $k$ -noncrossing structures. They coincide with noncrossing diagrams having minimum arc-length two.

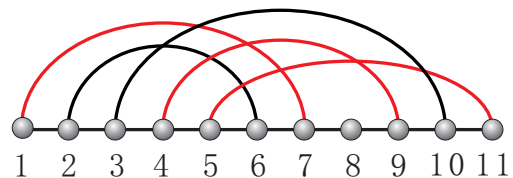


Figure 5:  $k$ -noncrossing diagrams: we display a 4-noncrossing diagram containing the three mutually crossing arcs  $(1, 7)$ ,  $(4, 9)$ ,  $(5, 11)$  (drawn in red).

We call diagrams containing at most  $(k - 1)$ -crossings,  $k$ -noncrossing diagrams. RNA secondary structures have no crossings in their diagram representation, see Figure 3 and Figure 4, and are therefore 2-noncrossing diagrams. A structure in which any stack has at least size  $\sigma$  is called  $\sigma$ -canonical, where a stack of size  $\sigma$  is a sequence of “parallel” arcs of the form

$$((i, j), (i+1, j-1), \dots, (i+(\sigma-1), j-(\sigma-1))). \quad (1)$$

As a natural generalization of RNA secondary structures  $k$ -noncrossing RNA structures [28–30] were introduced. A  $k$ -noncrossing RNA structure

is  $k$ -noncrossing diagram without arcs of the form  $(i, i+1)$ . In the following we assume  $k = 3$ , i.e. in the diagram representation there are at most two mutually crossing arcs, a minimum arc-length of four and a minimum stack-size of three base pairs. The notion  $k$ -noncrossing stipulates that the complexity of a pseudoknot is related to the maximal number of mutually crossing bonds. Indeed, most natural RNA pseudoknots are 3-noncrossing [31].

## 1.2 Neutral networks

Before considering an inverse folding algorithm into specific RNA structures one has to have at least some rationale as to why there exists *one* sequence realizing a given target as mfe-configuration. In fact this is, on the level of entire folding maps, guaranteed by the combinatorics of the target structures alone. It has been shown in [32], that the numbers of 3-noncrossing RNA pseudoknot structures, satisfying the biophysical constraints grows asymptotically as  $c_3 n^{-5} 2.03^n$ , where  $c_3 > 0$  is some explicitly known constant. In view of the central limit theorems of [33], this fact implies the existence of extended (exponentially large) sets of sequences that all fold into one 3-noncrossing RNA pseudoknot structure,  $S$ . In other words, the combinatorics of 3-noncrossing RNA structures alone implies that there are many sequences mapping (folding) into a single structure. The set of all such sequences is called the neutral network<sup>1</sup> of the structure  $S$  [34, 35], see Figure 6.

<sup>1</sup>the term “neutral network” as opposed to “neutral set” stems from giant component results of random induced sub-

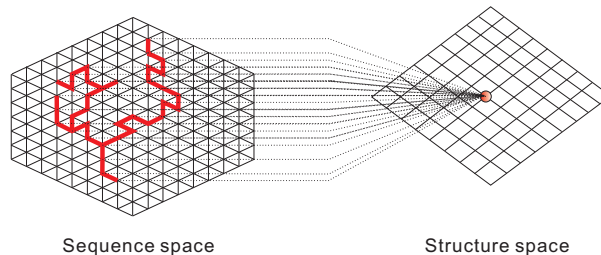


Figure 6: Neutral networks in sequence space: we display sequence space (left) and structure space (right) as grids. We depict a set of sequences that all fold into a particular structure. Any two of these sequences are connected by a red edge. The neutral network of this fixed structure consists of all sequences folding into it and is typically a connected subgraph of sequence space.

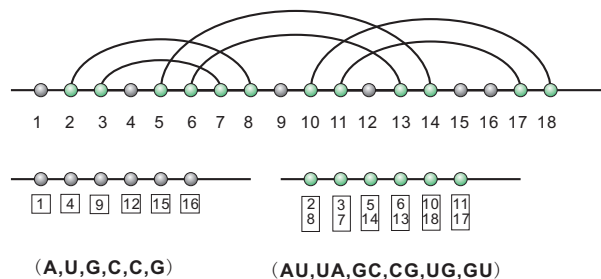


Figure 7: A structure and a particular compatible sequence organized in the segments of unpaired and paired bases.

By construction, all the sequences contained in such a neutral network are all compatible with  $S$ . That is, at any two positions paired in  $S$ , we find two bases capable of forming a bond (**A-U**, **U-A**, **G-C**, **C-G**, **G-U** and **U-G**), see Figure 7. Let  $s'$  be a sequence derived via a mutation<sup>2</sup> of  $s$ . If  $s'$  is again compatible with  $S$ , we call this mutation “compatible”.

Let  $C[S]$  denote the set of  $S$ -compatible sequences. The structure  $S$  motivates to consider a new adjacency relation within  $C[S]$ . Indeed, we may

graphs of  $n$ -cubes. That is, neutral networks are typically connected in sequence space

<sup>2</sup>note: we do not consider insertions or deletions.

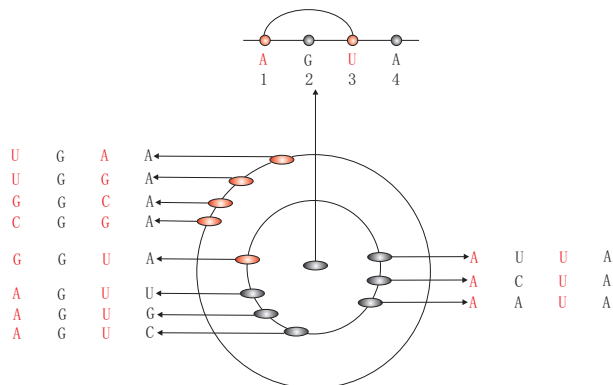


Figure 8: Diagram representation of an RNA structure (top) and its induced compatible neighbors in sequence space (bottom). Here the neighbors on the inner circle have Hamming distance one while those on the outer circle have Hamming distance two. Note that each base pair gives rise to five compatible neighbors (red) exactly one of which being in Hamming distance one.

reorganize a sequence  $(s_1, \dots, s_n)$  into the pair

$$\left( (u_1, \dots, u_{n_u}), (p_1, \dots, p_{n_p}) \right), \quad (2)$$

where the  $u_h$  denotes the unpaired nucleotides and the  $p_h = (s_i, s_j)$  denotes base pairs, respectively, see Figure 7. We can then view  $s_u = (u_1, \dots, u_{n_u})$  and  $s_p = (p_1, \dots, p_{n_p})$  as elements of the formal cubes  $Q_4^{n_u}$  and  $Q_6^{n_p}$ , implying the new adjacency relation for elements of  $C[S]$ .

Accordingly, there are two types of compatible neighbors in the sequence space **u**- and **p**-neighbors: a **u**-neighbor has Hamming distance one and differs exactly by a point mutation at an unpaired position. Analogously a **p**-neighbor differs by a compensatory base pair-mutation, see Figure 8.

Note, however, that a **p**-neighbor has either Hamming distance one (**G-C**  $\mapsto$  **G-U**) or Hamming distance two (**G-C**  $\mapsto$  **C-G**). We call a **u**- or a **p**-

neighbor,  $y$ , a compatible neighbor. In light of the adjacency notion for the set of compatible sequences we call the set of all sequences folding into  $S$  the neutral network of  $S$ . By construction, the neutral network of  $S$  is contained in  $C[S]$ . If  $y$  is contained in the neutral network we refer to  $y$  as a neutral neighbor. This gives rise to consider the compatible and neutral distance of the two sequences, denoted by  $C(s, s')$  and  $N(s, s')$ . These are the minimum length of a  $C[S]$ -path and path in the neutral network between  $s$  and  $s'$ , respectively. Note that since each neutral path is in particular a compatible path, the compatible distance is always smaller or equal than the neutral distance.

In this paper we study the inverse folding problem for RNA pseudoknot structures: for a given 3-noncrossing target structure  $S$ , we search for sequences from  $C[S]$ , that have  $S$  as mfe configuration.

## 2 Background

For RNA secondary structures, there are three different strategies for inverse folding, **RNAinverse**, **RNA-SSD** and **INFO-RNA** [36–38],

They all generate via a local search routine iteratively sequences, whose structures have smaller and smaller distances to a given target. Here the distance between two structures is obtained by aligning them as diagrams and counting “0”, if a given position is either unpaired or incident to an arc contained in both structures and “1”, otherwise, see Figure 9.

One common assumption in these inverse fold-

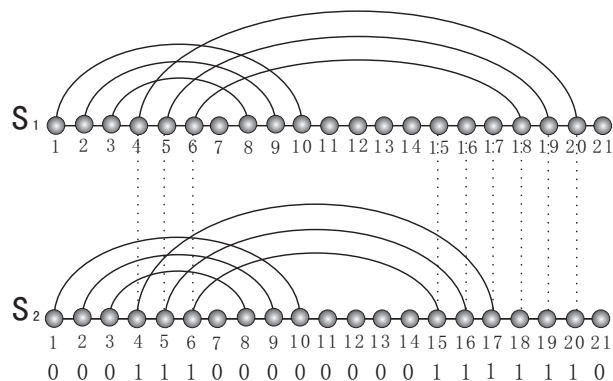


Figure 9: Positions paired differently in  $S_1$  and  $S_2$  are assigned a “1”. There are two types of positions: **I.**  $p$  is contained in different arcs, see position 4,  $(4, 20) \in S_1$  and  $(4, 17) \in S_2$ . **II.**  $p$  is unpaired in one structure and  $p$  is paired in the other, such as position 18.

ing algorithms is, that the energies of specific substructures contribute additively to the energy of the entire structure. Let us proceed by analyzing the algorithms.

**RNAinverse** is the first inverse-folding algorithm that derives sequences that realize given RNA secondary structures as mfe-configuration. In its initialization step, a random compatible sequence  $s$  for the target  $T$  is generated. Then **RNAinverse** proceeds by updating the sequence  $s$  to  $s', s'' \dots$  step by step, minimizing the structure distance between the mfe structure of  $s'$  and the target structure  $T$ . Based on the observation, that the energy of a substructure contributes additively to the mfe of the molecule, **RNAinverse** optimizes “small” substructures first, eventually extending these to the entire structure. While optimizing substructures, **RNAinverse** does an adaptive walk in order to decrease the structure distance. In fact, this walk is based entirely on ran-

dom compatible mutations.

**RNA-SSD** **RNA-SSD** first assigns specific probabilities to the bases located in unpaired positions and the base pairs (**G-C**, **A-U**, **U-G**) of  $T$ , respectively. In this assignment the probability of a unpaired position being assigned either A or U is greater than assigning G or C. Similarly, the probability of pairs **G-C** and **C-G** base pairs is greater than that of the other base pairs. Then, **RNA-SSD** derives a hierarchical decomposition of the target structure. It recursively splits the structure and thereby derives a binary decomposition tree rooted in  $T$  and whose leaves correspond to  $T$ -substructures. Each non-leaf node of this tree represents a substructure obtained by merging the two substructures of its respective children. Given this tree, **RNA-SSD** performs a stochastic local search, starting at the leaves, subsequently working its way up to the root.

**INFO-RNA** employs a dynamic programming method for finding a well suited initial sequence. This sequence has a lowest energy with respect to the  $T$ . Since the latter does not necessarily fold into  $T$ , (due to potentially existing competing configurations) **INFO-RNA** then utilizes an improved<sup>3</sup> stochastic local search in order to find a sequence in the neutral network of  $T$ . In contrast to **RNAinverse**, **INFO-RNA** allows for increasing the distance to the target structure. At the same time, only positions that do not pair correctly and

<sup>3</sup>relative to the local search routine used in **RNAinverse**

positions adjacent to these are examined.

## 2.1 Cross

**Cross** is an *ab initio* folding algorithm that maps RNA sequences into 3-noncrossing RNA structures. It is guaranteed to search all 3-noncrossing,  $\sigma$ -canonical structures and derives some (not necessarily unique), loop-based mfe-configuration. In the following we always assume  $\sigma \geq 3$ . The input of **Cross** is an arbitrary RNA sequence  $s$  and an integer  $N$ . Its output is a list of  $N$  3-noncrossing,  $\sigma$ -canonical structures, the first of which being the mfe-structure for  $s$ . This list of  $N$  structures  $(C_0, C_1, \dots, C_{N-1})$  is ordered by the free energy and the first list-element, the mfe-structure, is denoted by  $\mathbf{Cross}(s)$ . If no  $N$  is specified, **Cross** assumes  $N = 1$  as default.

**Cross** generates a mfe-structure based on specific loop-types of 3-noncrossing RNA structures. For a given structure  $S$ , let  $\alpha$  be an arc contained in  $S$  ( $S$ -arc) and denote the set of  $S$ -arcs that cross  $\alpha$  by  $\mathcal{A}_S(\alpha)$ .

For two arcs  $\alpha = (i, j)$  and  $\alpha' = (i', j')$ , we next specify the partial order “ $\prec$ ” over the set of arcs:

$$\alpha' \prec \alpha \quad \text{if and only if} \quad i < i' < j' < j.$$

All notions of minimal or maximal elements are understood to be with respect to  $\prec$ . An arc  $\alpha \in \mathcal{A}_S(\beta)$  is called a minimal,  $\beta$ -crossing if there exists no  $\alpha' \in \mathcal{A}_S(\beta)$  such that  $\alpha' \prec \alpha$ . Note that  $\alpha \in \mathcal{A}_S(\beta)$  can be minimal  $\beta$ -crossing, while  $\beta$  is not minimal  $\alpha$ -crossing. 3-noncrossing diagrams exhibit the fol-

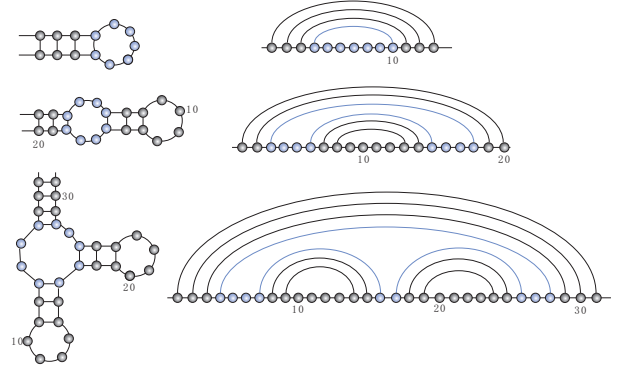


Figure 10: The standard loop-types: hairpin-loop (top), interior-loop (middle) and multi-loop (bottom). These represent all loop-types that occur in RNA secondary structures.

lowing four basic loop-types:

- (1) A hairpin-loop is a pair

$$((i, j), [i + 1, j - 1])$$

where  $(i, j)$  is an arc and  $[i, j]$  is an interval, i.e. a sequence of consecutive vertices  $(i, i + 1, \dots, j - 1, j)$ .

- (2) An interior-loop, is a sequence

$$((i_1, j_1), [i_1 + 1, i_2 - 1], (i_2, j_2), [j_2 + 1, j_1 - 1]),$$

where  $(i_2, j_2)$  is nested in  $(i_1, j_1)$ . That is we have  $i_1 < i_2 < j_2 < j_1$ .

- (3) A multi-loop, see Figure 10 [20], is a sequence

$$((i_1, j_1), [i_1 + 1, \omega_1 - 1], S_{\omega_1}^{\tau_1}, [\tau_1 + 1, \omega_2 - 1], S_{\omega_2}^{\tau_2}, \dots),$$

where  $S_{\omega_h}^{\tau_h}$  denotes a pseudoknot structure over  $[\omega_h, \tau_h]$  (i.e. nested in  $(i_1, j_1)$ ) and subject to the following condition: if all  $S_{\omega_h}^{\tau_h} = (\omega_h, \tau_h)$ , i.e. all substructures are just arcs, for all  $h$ , then we have  $h \geq 2$ .

A pseudoknot, see Figure 11 [20], consists of the following data:

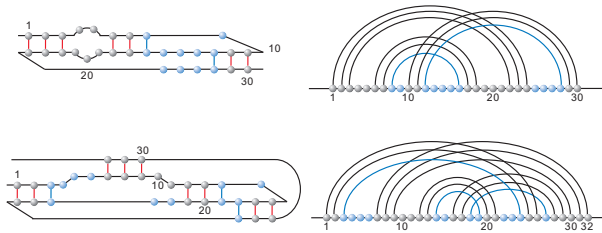


Figure 11: Pseudoknot loops, formed by all blue vertices and arcs.

(P1) A set of arcs

$$P = \{(i_1, j_1), (i_2, j_2), \dots, (i_t, j_t)\},$$

where  $i_1 = \min\{i_h\}$  and  $j_t = \max\{j_h\}$ , such that

- (i) the diagram induced by the arc-set  $P$  is irreducible, i.e. the dependency-graph of  $P$  (i.e. the graph having  $P$  as vertex set and in which  $\alpha$  and  $\alpha'$  are adjacent if and only if they cross) is connected and
- (ii) for each  $(i_h, j_h) \in P$  there exists some arc  $\beta$  (not necessarily contained in  $P$ ) such that  $(i_h, j_h)$  is minimal  $\beta$ -crossing.

(P2) Any  $i_1 < x < j_t$ , not contained in hairpin-, interior- or multi-loops.

Having discussed the basic loop-types, we are now in position to state

**Theorem 1** *Any 3-noncrossing RNA pseudoknot structure has a unique loop-decomposition [20].*

Figure 12 illustrates the loop decomposition of a 3-noncrossing structure.

A **motif** in **Cross** is a 3-noncrossing structure, having only  $\prec$ -maximal stacks of size exactly  $\sigma$ , see

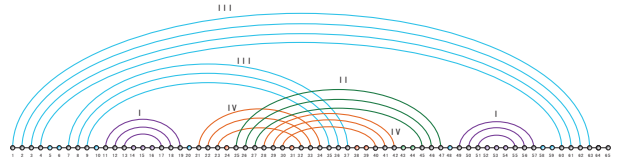


Figure 12: Loop decomposition: here a hairpin-loop (I), an interior-loop (II), a multi-loop (III) and a pseudoknot (IV).

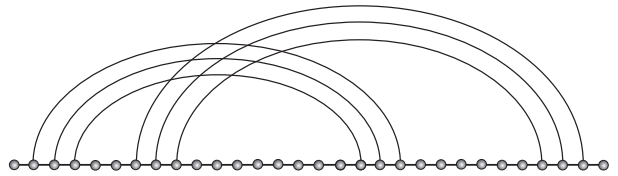


Figure 13: Motif: a 3-noncrossing, 3-canonical motif.

Figure 13. A **skeleton**,  $S$ , is a  $k$ -noncrossing structure such that

- its core,  $c(S)$  has no noncrossing arcs and
- its  $L$ -graph,  $L(S)$  is connected.

Here the core of a structure,  $c(S)$ , is obtained by collapsing its stacks into single arcs (thereby reducing its length) and the graph  $L(S)$  is obtained by mapping arcs into vertices and connecting any two if they cross in the diagram representation of  $S$ , see Figure 14. As for the general strategy, **Cross** constructs 3-noncrossing RNA structure “from top to bottom” via three subroutines:

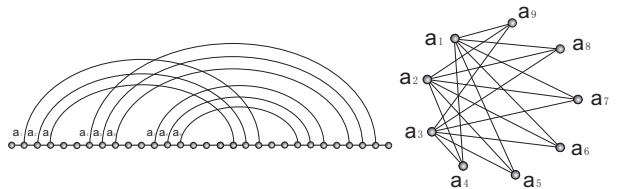


Figure 14: Skeleton and its  $L$ -graph: we display a skeleton (left) and its  $L$ -graph (right).



**I (SHADOW):** Here we generate all maximal stacks of the structure. Note that a stack is maximal with respect to  $\prec$  if it is not nested in some other stack. This is derived by “shadowing” the motifs, i.e. their  $\sigma$ -stacks are extended “from top to bottom”.

**II (SKELETONBRANCH):** Given a shadow, the second step of **Cross** consists in generating, the skeleton-tree. The nodes of this tree are particular 3-noncrossing structures, obtained by successive insertions of stacks. Intuitively, a skeleton encapsulates all cross-serial arcs that cannot be recursively computed. Here the tree complexity is controlled via limiting the (total) number of pseudoknots.

**III (SATURATION):** In the third subroutine each skeleton is saturated via DP-routines. After the saturation the mfe-3-noncrossing structure is derived.

Figure 15 provides an overview on how the three subroutines are combined.

### 3 The algorithm

The inverse folding algorithm **Inv** is based on the *ab initio* folding algorithm **Cross**. The input of **Inv** is the target structure,  $T$ . The latter is expressed as a character string of “:()[]{}”, where “:” denotes unpaired base and “()”, “[ ]”, “{ }” denote paired bases.

In Algorithm 1, we present the pseudocodes of algorithm **Inv**. After validation of the target structure (lines 2 to 5 in Algorithm 1), similar to **INFO-RNA**, **Inv** constructs an initial sequence and then proceeds

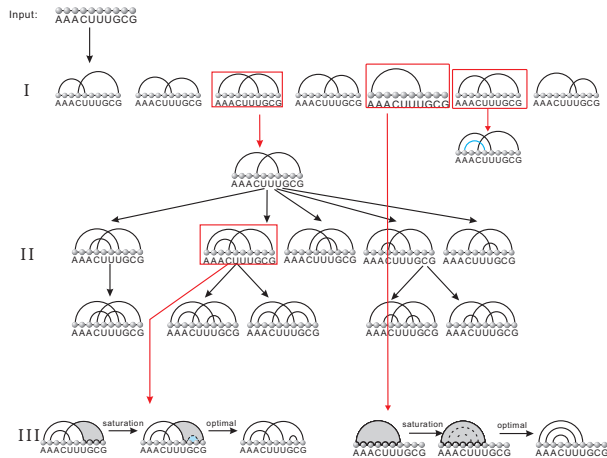


Figure 15: An outline of **Cross** (for illustration purposes we assume here  $\sigma = 1$ ): The routines **SHADOW**, **SKELETONBRANCH** and **SATURATION** are depicted. Due to space limitations we only represent a few select motifs and for the same reason only one of the motifs displayed in the first row is extended by one arc (drawn in blue). Furthermore note that only motifs with crossings give rise to nontrivial skeleton-trees, all other motifs are considered directly as input for **SATURATION**.

by a stochastic local search based on the loop decomposition of the target. This sequence is derived via the routine **ADJUST-SEQ**. We then decompose the target structure into loops and endow these with a linear order. According to this order we use the routine **LOCAL-SEARCH** in order to find for each loop a “proper” local solution.

#### 3.1 ADJUST-SEQ

In this section we describe Steps 2 and 3 of the pseudocodes presented in Algorithm 1. The routine **MAKE-START**, see line 8, generates a random sequence,  $start$ , which is compatible to the target, with uniform probability.

We then initialize the variable  $seq_{\min}$  via the sequence  $start$  and set the variable  $d = +\infty$ ,

---

**Algorithm 1** Inv

---

**Input:**  $k$ -noncrossing target structure  $T$ **Output:** an RNA sequence  $seq$ **Require:**  $k \leq 3$  and  $T$  is composed with “:()[]{}”**Ensure:**  $\text{Cross}(seq) = T$ 

```
1: ▷ Step 1: Validate structure
2: if false = CHECK-STRU( $T$ ) then
3:   print incorrect structure
4:   return NIL
5: end if
6:
7: ▷ Step 2: Generate the start sequence
8:  $start \leftarrow$  MAKE-START( $T$ )
9:
10: ▷ Step 3: Adjust the start sequence
11:  $seq_{\text{middle}} \leftarrow$  ADJUST-SEQ( $start, T$ )
12:
13: ▷ Step 4: Decompose  $T$  and derive the ordered intervals.
14: Interval array  $I$ 
15:  $m \leftarrow |I|$  ▷  $I$  satisfies  $I_m = T$ 
16:
17: ▷ Step 5: Stochastic Local Search
18:  $seq \leftarrow seq_{\text{middle}}$ 
19: for all intervals in the array  $I_w$  do
20:    $l \leftarrow$  start-point( $I_w$ )
21:    $r \leftarrow$  end-point( $I_w$ )
22:    $s' \leftarrow seq|_{[l,r]}$  ▷ get sub-sequence
23:    $seq|_{[l,r]} \leftarrow$  LOCAL-SEARCH( $s', I_w$ )
24: end for
25:
26: ▷ Step 6: output
27: if  $seq_{\text{min}} = \text{Cross}(seq)$  then
28:   return  $seq$ 
29: else
30:   print Failed!
31:   return NIL
32: end if
```

---

where  $d$  denotes the structure distance between  $\text{Cross}(seq_{\text{min}})$  and  $T$ .

Given the sequence  $start$ , we construct a set of potential “competitors”,  $C$ , i.e. a set of structures suited as folding targets for  $start$ . In Algorithm 2 we show how to adjust the start sequence using the routine ADJUST-SEQ. Lines 4 to 38 of Algorithm 2, contain a **For**-loop, executed at most  $\sqrt{n}/2$  times. Here the loop-length  $\sqrt{n}/2$  is heuristically determined.

Setting the **Cross**-parameter<sup>4</sup>,  $N$ , the subroutine executed in the loop-body consists of the following three steps.

**Step I. Generating  $C^0(\lambda^i)$  via **Cross**.** Suppose we are in the  $i$ th step of the **For**-loop and are given the sequence  $\lambda^{i-1}$  where  $\lambda^0 = start$ . We consider  $\text{Cross}(\lambda^{i-1}, N)$ , i.e. the list of suboptimal structures with respect to  $\lambda^{i-1}$ ,

$$C^0(\lambda^{i-1}) = \text{Cross}(\lambda^{i-1}, N) = (C_h^0(\lambda^{i-1}))_{h=0}^{N-1}$$

If  $C_0^0(\lambda^{i-1}) = T$ , then **Inv** returns  $\lambda^{i-1}$ . Else, in case of  $d = (\text{Cross}(C_0^0(\lambda^{i-1})), T) < d_{\text{min}}$ , we set

$$\begin{aligned} seq_{\text{min}} &= \lambda^{i-1} \\ d_{\text{min}} &= d(\text{Cross}(C_0^0(\lambda^{i-1})), T). \end{aligned}$$

Otherwise we do not update  $seq_{\text{min}}$  and go directly to Step II.

**Step II. The competitors.** We introduce a specific procedure that “perturbs” arcs of a given RNA pseudo-knot structure,  $S$ . Let  $a$  be an arc of  $S$  and let  $l(a)$ ,  $r(a)$  denote the start- and end-point of  $a$ . A pertur-

---

<sup>4</sup>For all computer experiments we set  $N = 50$ .

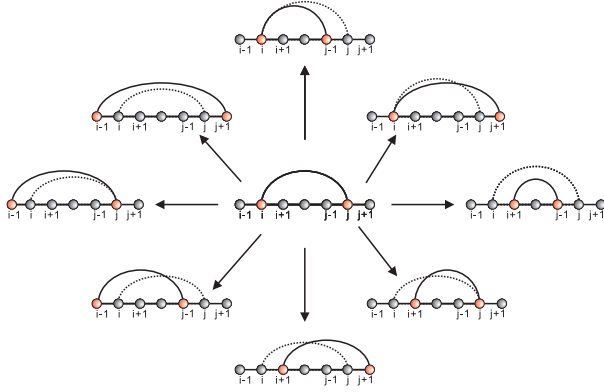


Figure 16: Nine perturbations of an arc  $(i, j)$ . Original arcs are drawn dotted, and the arcs incident to red bases are the perturbations.

bation of  $a$  is a procedure which generates a new arc  $a'$ , such that

$$|l(a) - l(a')| \leq 1 \quad \text{and} \quad |r(a) - r(a')| \leq 1.$$

Clearly, there are nine perturbations of any given arc  $a$  (including  $a$  itself), see Figure 16.

We proceed by keeping  $a$ , replacing the arc  $a$  by a nontrivial perturbation or remove  $a$ , arriving at a set of ten structures  $\nu(S, a)$ .

Now we use this method in order to generate the set  $C^1(\lambda^{i-1})$  by perturbing each arc of each structure  $C_h^0(\lambda^{i-1}) \in C^0(\lambda^{i-1})$ . If  $C_h^0(\lambda^{i-1})$  has  $A_h$  arcs,  $\{a_h^1, \dots, a_h^{A_h}\}$ , then

$$C^1(\lambda^{i-1}) = \bigcup_{h=0}^{N-1} \bigcup_{j=1}^{A_h} \nu(C_h^0(\lambda^{i-1}), a_h^j).$$

This construction may result in duplicate, inconsistent or incompatible structures. Here, a structure is inconsistent if there exists at least one position paired with more than one base, and incompatible if there exists at least one arc not compatible with  $\lambda^{i-1}$ , see Figures 17 and 18. Here compatibility is

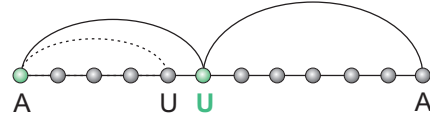


Figure 17: Inconsistent structures: the dotted arc is perturbed by shifting its end-point. This perturbation leads to a nucleotide establishing two base pairs, which is impossible.

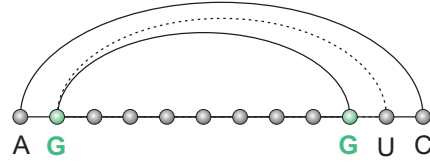


Figure 18: Incompatible structures: we display a perturbation of the dotted arc leading to a structure that is incompatible to the given sequence.

understood with respect to the Watson-Crick and **G-U** base pairing rules. Deleting inconsistent and incompatible structures, as well as those identical to the target, we arrive at the set of competitors,

$$C(\lambda^{i-1}) \subset C^1(\lambda^{i-1}).$$

**Step III. Mutation** Here we adjust  $\lambda^{i-1}$  with respect to  $T$  as well as the set of competitors,  $C(\lambda^{i-1})$  derived in the previous step. Suppose  $\lambda^{i-1} =$

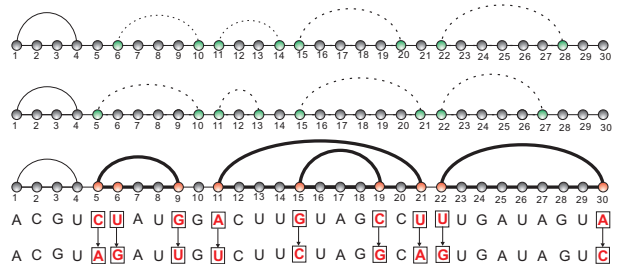


Figure 19: Mutation: Suppose the top and middle structures represent the set of competitors and the bottom structure is target. We display  $\lambda^{i-1}$  (top sequence) and its mutation,  $\lambda^i$  (bottom sequence). Two nucleotides of base pairs not contained in  $T$  are colored green, nucleotides subject to mutations are colored red.

$s_1^{i-1} s_2^{i-1} \dots s_n^{i-1}$ . Let  $p(S, w)$  be the position paired to the position  $w$  in the RNA structure  $S \in C(\lambda^{i-1})$ , or 0 if position  $w$  is unpaired. For instance, in Figure 19, we have  $p(T, 1) = 4$ ,  $p(T, 2) = 0$  and  $p(T, 4) = 1$ . For each position  $w$  of the target  $T$ , if there exists a structure  $C_h(\lambda^{i-1}) \in C(\lambda^{i-1})$  such that  $p(C_h(\lambda^{i-1}), w) \neq p(T, w)$  (see positions 5, 6, 9, and 11 in Figure 19) we modify  $\lambda^{i-1}$  as follows:

1. **unpaired position:** If  $p(T, w) = 0$ , we update  $s_w^{i-1}$  randomly into the nucleotide  $s_w^i \neq s_w^{i-1}$ , such that for each  $C_h(\lambda^{i-1}) \in C(\lambda^{i-1})$ , either  $p(C_h(\lambda^{i-1}), w) = 0$  or  $s_w^i$  is not compatible with  $s_v^{i-1}$  where  $v = p(C_h(\lambda^{i-1}), w) > 0$ . See position 6 in Figure 19.
2. **start-point:** If  $p(T, w) > w$ , set  $v = p(T, w)$ . We randomly choose a compatible base pair  $(s_w^i, s_v^i)$  different from  $(s_w^{i-1}, s_v^{i-1})$ , such that for each  $C_h(\lambda^{i-1}) \in C(\lambda^{i-1})$ , either  $p(C_h(\lambda^{i-1}), w) = 0$  or  $s_w^i$  is not compatible with  $s_u^{i-1}$ , where  $u = p(C_h(\lambda^{i-1}), w) > 0$  is the end-point paired with  $s_w^{i-1}$  in  $C_h(\lambda^{i-1})$  (Figure 19: (5, 9)). The pair **G-C** retains the compatibility to (5, 9), but is incompatible to (5, 10)). By Figure 20 we show feasibility of this step.
3. **end-point:** If  $0 < p(T, w) < w$ , then by construction the nucleotide has already been considered in the previous step.

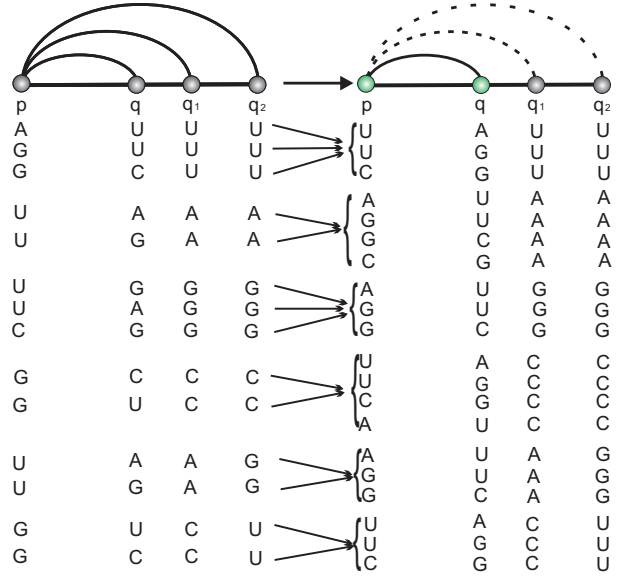


Figure 20: Mutations are always possible: suppose  $p$  is paired with  $q$  in  $T$  and  $p$  is paired with  $q_1$  in one competitor and  $q_2$  in another one. For a fixed nucleotide at  $p$  there are at most two scenarios, since a base can pair with at most two different bases. For instance, for **G** we have the pairs **G-C**, **G-U**. We display all nucleotide configurations (LHS) and their corresponding solutions (RHS).

Therefore, updating all the nucleotides of  $\lambda^{i-1}$ , we arrive at the new sequence  $\lambda^i = s_1^i s_2^i \dots s_n^i$ .

Note that the above mutation steps heuristically decrease the structure distance. However, the resulting sequence is not necessarily incompatible to all competitors. For instance, consider a competitor  $C_h$  whose arcs are all contained  $T$ . Since  $\lambda^i$  is compatible with  $T$ ,  $\lambda^i$  is compatible with  $C_h$ . Since competitors are obtained from suboptimal folds such a scenario may arise.

In practice, this situation represents not a problem, since these type of competitors are likely to be ruled out by virtue of the fact that they have a mfe larger than that of the target structure.

Accordingly we have the following situation, competitors are eliminated due to two, equally important criteria: incompatibility as well as minimum free energy considerations.

If the distance of  $\text{Cross}(\lambda^i)$  to  $T$  is less than or equal to  $d_{\min} + 5$ , we return to Step I (with  $\lambda^i$ ). Otherwise, we repeat Step III (for at most 5 times) thereby generating  $\lambda_1^i, \dots, \lambda_5^i$  and set  $\lambda^i = \lambda_w^i$  where  $d(\text{Cross}(\lambda_w^i), T)$  is minimal.

The procedure ADJUST-SEQ employs the negative paradigm [17] in order to exclude energetically close conformations. It returns the sequence  $seq_{\text{middle}}$  which is tailored to realize the target structure as mfe-fold.

---

### Algorithm 2 ADJUST-SEQ

---

**Input:** the original start sequence  $start$

**Input:** the target structure  $T$

**Output:** a initialized sequence  $seq_{\text{middle}}$

```

1:  $n \leftarrow$  length of  $T$ 
2:  $d_{\min} \leftarrow +\infty$ ,  $seq_{\min} \leftarrow start$ 
3: for  $i = 1$  to  $\frac{1}{2}\sqrt{n}$  do
4:    $\triangleright$  Step I: generate the set  $C^0(\lambda^{i-1})$  via Cross
5:    $C^0(\lambda^{i-1}) \leftarrow \text{Cross}(\lambda^{i-1}, N)$ 
6:    $d \leftarrow d(C_0^0(\lambda^{i-1}), T)$ 
7:   if  $d = 0$  then
8:     return  $\lambda^{i-1}$ 
9:   else if  $d < d_{\min}$  then
10:     $d_{\min} \leftarrow d$ ,  $seq_{\min} \leftarrow \lambda^{i-1}$ 
11:   end if
12:
13:    $\triangleright$  Step II: generate the competitor set  $C(\lambda^{i-1})$ 
14:    $C^1(\lambda^{i-1}) \leftarrow \phi$ 
15:   for all  $C_h^1(\lambda^{i-1}) \in C^1(\lambda^{i-1})$  do
16:     for all arc  $a_h^j$  of  $C_h^1(\lambda^{i-1})$  do
17:        $C^1(\lambda^{i-1}) \leftarrow C^1(\lambda^{i-1}) \cup \nu(C_0^1(\lambda^i), a_h^j)$ 
18:     end for
19:   end for
20:    $C(\lambda^{i-1}) =$ 
21:    $\{C_h^1(\lambda^{i-1}) \in C^1(\lambda^{i-1}) : C_h^1(\lambda^{i-1}) \text{ is valid}\}$ 
22:
23:    $\triangleright$  Step III: mutation
24:    $seq \leftarrow \lambda^{i-1}$ 
25:   for  $w = 1$  to  $n$  do
26:     if  $\exists C_h(\lambda^{i-1}) \in C(\lambda^{i-1})$  s.t.  $p(C_h, w) \neq p(T, w)$ 
27:       then
28:          $seq[w] \leftarrow$  random nucleotide or pair, s.t.
29:          $\forall C_h(\lambda^{i-1}) \in C(\lambda^{i-1})$ ,  $seq \in C[T]$  and  $seq \notin$ 
30:          $C[C_h(\lambda^{i-1})]$ .
31:       end if
32:     end for
33:    $T_{seq} \leftarrow \text{Cross}(seq)$ 
34:   if  $d(T_{seq}, T) < d_{\min} + 5$  then
35:      $seq_{\text{middle}} \leftarrow seq$ 
36:   else if Step III run less than 5 times then
37:     goto Step III
38:   end if
39: end for  $\triangleright$  loop to line 3
40: return  $seq_{\text{middle}}$ 

```

---

### 3.2 DECOMPOSE and LOCAL-SEARCH

In this section we introduce two the routines, DECOMPOSE and LOCAL-SEARCH. The routine DECOMPOSE partitions  $T$  into linearly ordered energy independent components, see Figure 12 and Section 2.1. LOCAL-SEARCH constructs iteratively an optimal sequence for  $T$  via local solutions, that are optimal to certain substructures of  $T$ .

DECOMPOSE: Suppose  $T$  is decomposed as follows,

$$B = \{T_1, \dots, T_{m'}\}.$$

where the  $T_w$  are the loops together with all arcs in the associated stems of the target.

We define a linear order over  $B$  as follows:  $T_w < T_h$  if either

1.  $T_w$  is nested in  $T_h$ , or
2. the start-point of  $T_w$  precedes that of  $T_h$ .

In Figure 21 we display the linear order of the loops of the structure shown in Figure 12.

Next we define the interval

$$a_w = [l(T_w), r(T_w)] \quad 1 \leq w \leq m',$$

projecting the loop  $T_w$  onto the interval  $[l(T_w), r(T_w)]$  and  $b_w = [l', r'] \supset a_w$ , being the maximal interval consisting of  $a_w$  and its adjacent unpaired consecutive nucleotides, see Figure 12. Given two consecutive loops  $T_w < T_{w+1}$ , we have two scenarios:

- either  $b_w$  and  $b_{w+1}$  are adjacent, see  $b_5$  and  $b_6$  in Figure 21,

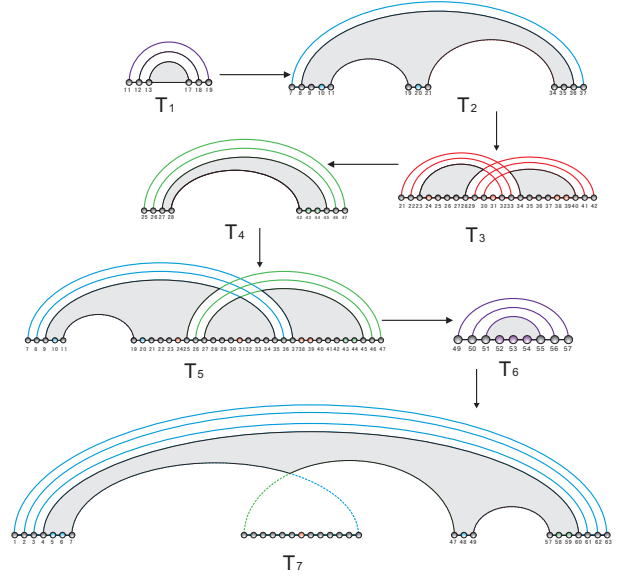


Figure 21: Linear ordering of loops:  $a_1 = [11, 19]$ ,  $b_1 = [10, 20]$ ,  $a_2 = [7, 37]$ ,  $b_2 = [5, 39]$ ,  $a_3 = [21, 42]$ ,  $b_3 = [20, 44]$ ,  $a_4 = [25, 47]$ ,  $b_4 = [24, 48]$ ,  $a_5 = [7, 47]$ ,  $b_5 = [5, 48]$ ,  $a_6 = [49, 57]$ ,  $b_6 = [48, 59]$ ,  $a_7 = [1, 63]$ ,  $b_7 = [1, 65]$ .

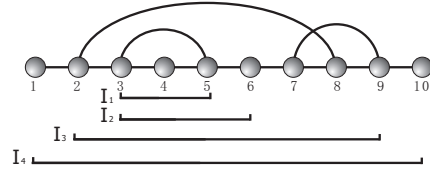


Figure 22: Loops and their induced sequence of intervals.

- or  $b_w \subseteq b_{w+1}$ , see  $b_1$  and  $b_2$  in Figure 21.

Let  $c_w = \cup_{h=1}^w b_h$ , then we have the sequence of intervals  $a_1, b_1, c_1, \dots, a_{m'}, b_{m'}, c_{m'}$ . If there are no unpaired nucleotides adjacent to  $a_w$ , then  $a_w = b_w$  and we simply delete all such  $b_w$ . Thereby we derive the sequence of intervals  $I_1, I_2, \dots, I_m$ . In Figure 22 we illustrate how to obtain this interval sequence: here the target decomposes into the loops  $T_1, T_2$  and we have  $I_1 = [3, 5]$ ,  $I_2 = [3, 6]$ ,  $I_3 = [2, 9]$ , and  $I_4 = [1, 10]$ .

LOCAL-SEARCH: Given the sequence of intervals  $I_1, I_2, \dots, I_m$ . We proceed by performing a local stochastic search on the subsequences  $seq|_{I_1}, seq|_{I_2}, \dots, seq|_{I_m}$  (initialized via  $seq = seq_{\text{middle}}$  and where  $s|_{[x,y]} = s_x s_{x+1} \dots s_y$ ). When we perform the local search on  $seq|_{I_w}$ , only positions that contribute to the distance to the target, see Figure 9, or positions adjacent to the latter, will be altered. We use the arrays  $U_1, U_2$  to store the unpaired and paired positions of  $T$ . In this process, we allow for mutations that increase the structure distance by five with probability 0.1. The latter parameter is heuristically determined. We iterate this routine until the distance is either zero or some halting criterion is met.

## 4 Discussion

The main result of this paper is the presentation of the algorithm `Inv`, freely available at

<http://www.combinatorics.cn/cbpc/inv.html>

Its input is a 3-noncrossing RNA structure  $T$ , given in terms of its base pairs  $(i_1, i_2)$  (where  $i_1 < i_2$ ). The output of `Inv` is an RNA sequences  $s = (s_1 s_2 \dots s_n)$ , where  $s_h \in \{\mathbf{A}, \mathbf{C}, \mathbf{G}, \mathbf{G}\}$  with the property  $\text{Cross}(s) = T$ , see Figure 23.

The core of `Inv` is a stochastic local search routine which is based on the fact that each 3-noncrossing RNA structure has a unique loop-decomposition, see Theorem 1 in Section 2.1. `Inv` generates “optimal” subsequences and eventually ar-

---

### Algorithm 3 LOCAL-SEARCH

---

**Input:**  $seq_{\text{middle}}$   
**Input:** the target  $T$   
**Output:**  $seq$   
**Ensure:**  $\text{Cross}(seq) = T$

- 1:  $seq \leftarrow seq_{\text{middle}}$
- 2: **if**  $\text{Cross}(seq) = T$  **then**
- 3:     **return**  $seq$
- 4: **end if**
- 5: decompose  $T$  and derive the ordered intervals.
- 6:  $I \leftarrow [I_1, I_2, \dots, I_m]$
- 7: **for all**  $I_w$  in  $I$  **do**
- 8:      $\triangleright$  Phase I: Identify positions.
- 9:      $d_{\min} = d(\text{Cross}(seq|_{I_w}, T|_{I_w}))$     $\triangleright$  initialize  $d_{\min}$
- 10:
- 11:     derive  $U_1$  via  $\text{Cross}(seq|_{I_w}, T|_{I_w})$
- 12:     derive  $U_2$  via  $\text{Cross}(seq|_{I_w}, T|_{I_w})$
- 13:
- 14:      $\triangleright$  Phase II: Test and Update.
- 15:     **for all**  $p$  in  $U_1$  **do**
- 16:         random  $T$  compatible mutate  $seq_p$
- 17:     **end for**
- 18:     **for all**  $[p, q]$  in  $U_2$  **do**
- 19:         random  $T$  compatible mutate  $seq_p$
- 20:     **end for**
- 21:
- 22:      $E \leftarrow \phi$
- 23:     **for all**  $p \in U_1, U_2$  **do**
- 24:
- 25:          $d \leftarrow d(T, \text{Cross}(seq_p))$
- 26:         **if**  $d < d_{\min}$  **then**
- 27:              $d_{\min} \leftarrow d, \quad seq \leftarrow seq_p$
- 28:             **goto** Phase I
- 29:         **else if**  $d_{\min} < d < d_{\min} + 5$  **then**
- 30:             **goto** Phase I with the probability 0.1
- 31:         **end if**
- 32:         **if**  $d = d_{\min}$  **then**
- 33:              $E \leftarrow E \cup \{seq\}$
- 34:         **end if**
- 35:     **end for**
- 36:     **end for**
- 37:      $seq \leftarrow e_0 \in E$ , where  $e_0$  has the lowest mfe in  $E$
- 38:     **if** Phase I run less than  $10n$  times **then**
- 39:         **goto** Phase I
- 40:     **end if**
- 41: **end for**
- 42: **return**  $seq$

---

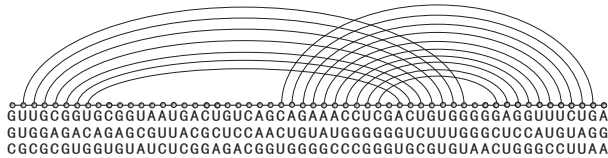


Figure 23: UTR pseudoknot of bovine coronavirus [39]: its diagram representation and three sequences of its neutral network as constructed by `Inv`.

rives at a global solution for  $T$  itself. `Inv` generalizes the existing inverse folding algorithm by considering arbitrary 3-noncrossing canonical pseudoknot structures. Conceptually, `Inv` differs from `INFO-RNA` in how the start sequence is being generated and the particulars of the local search itself.

As discussed in the introduction it has to be given an argument as to *why* the inverse folding of pseudoknot RNA structures works. While folding maps into RNA secondary structures are well understood, the generalization to 3-noncrossing RNA structures is nontrivial. However the combinatorics of RNA pseudoknot structures [28, 29, 40] implies the existence of large neutral networks, i.e. networks composed by sequences that all fold into a specific pseudoknot structure. Therefore, the fact that it is indeed possible to generate via `Inv` sequences contained in the neutral networks of targets against competing pseudoknot configurations, see Figure 23 and Figure 24 confirms the predictions of [32].

An interesting class are the 3-noncrossing nonplanar pseudoknot structures. A nonplanar pseudoknot structure is a 3-noncrossing structure which is not a bi-secondary structure in the sense of Stadler [31]. That is, it cannot be represented by non-

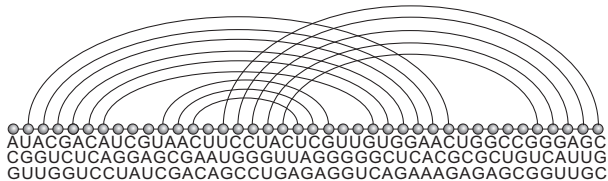


Figure 24: The Pseudoknot PKI of the internal ribosomal entry site (IRES) region [41]: its diagram representation and three sequences of its neutral network as constructed by `Inv`.

crossing arcs using the upper and lower half planes. Since DP-folding paradigms of pseudoknots folding are based on gap-matrices [16], the minimal class of “missed” structures<sup>5</sup> are exactly these, nonplanar, 3-noncrossing structures. In Figure 25 we showcase a nonplanar RNA pseudoknot structure and 3 sequences of its neutral network, generated by `Inv`.

As for the complexity of `Inv`, the determining factor is the subroutine `LOCAL-SEARCH`. Suppose that the target is decomposed into  $m$  intervals with the length  $\ell_1, \dots, \ell_m$ . For each interval, we may assume that line 2 of `LOCAL-SEARCH` runs for  $f_h$  times, and that line 14 is executed for  $g_h$  times. Since `LOCAL-SEARCH` will stop (line 4) if  $T_{start} = T$  (line 3), the remainder of `LOCAL-SEARCH`, i.e. lines 7 to 41 run for  $(f_h - 1)$  times, each such execution having complexity  $O(\ell_h)$ . Therefore we arrive at the complexity

$$\sum_{h=1}^m ((f_h + g_h) c(\ell_h) + (f_h - 1) O(\ell_h)),$$

where  $c(\ell)$  denotes the complexity of the `Cross`. The multiplicities  $f_h$  and  $g_h$  depend on various factors, such as *start*, the random order of the elements of

<sup>5</sup>given the implemented truncations



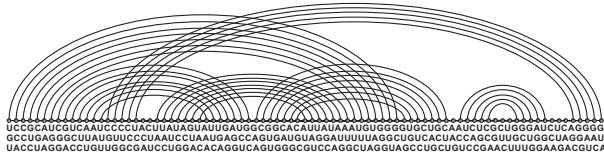


Figure 25: A nonplanar 3-noncrossing RNA structure together with three sequences realizing them as mfe-structures.

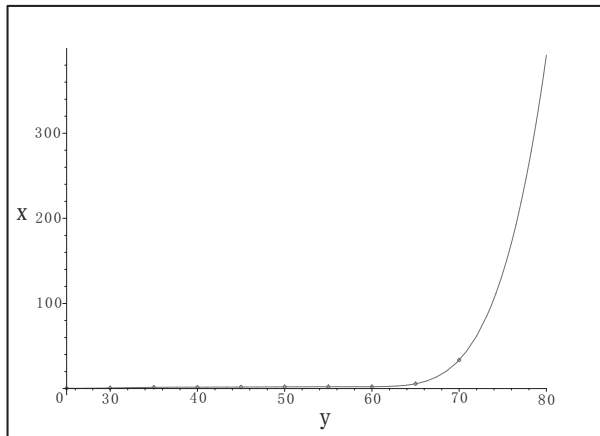


Figure 26: Approximation using 2 cubic spines fitting of mean inverse folding time (seconds) over sequence length. For  $n = 35, \dots, 75$  we choose a natural pseudoknot structure from the PKdatabase and display the average inverse folding time based on sampling 200 sequences of the neutral network of the respective target.

$U_1, U_2$  (see Algorithm 3) and the probability  $p$ . According to [33] the complexity of  $c(\ell_h)$  is  $O(e^{1.146 \ell_h})$  and accordingly the complexity of  $\text{Inv}$  is given by

$$\sum_{h=1}^m ((f_h + g_h) O(e^{1.146 \ell_h})).$$

In Figure 26 we present the average inverse folding time of several natural RNA structures taken from the PKdatabase [42]. These averages are computed via generating 200 sequences of the target’s neutral networks. In addition we present in Table 1 the total time for 100 executions of  $\text{Inv}$  for an additional set of RNA pseudoknot structures.

## 5 Competing interests

The authors declare that they have no competing interests.

## 6 Authors contributions

All authors contributed equally to this paper.

## 7 Acknowledgments

We are grateful to Fenix W.D. Huang for discussions. Special thanks belongs to the two anonymous referee’s whose thoughtful comments have greatly helped in deriving an improved version of the paper. This work was supported by the 973 Project, the PCSIRT of the Ministry of Education, the Ministry of Science and Technology, and the National Science Foundation of China.

## References

- Westhof E, Jaeger L: **RNA pseudoknots**. *Curr Opin Struct Biol* 1992, **2**(3):327–333.
- Loria A, Pan T: **Domain structure of the ribozyme from eubacterial ribonuclease P**. *RNA* 1996, **2**:551–563.
- Staple DW, Butcher SE: **Pseudoknots: RNA structures with diverse functions**. *PLoS Biol* 2005, **3**(6):e213.
- Konings DA, Gutell RR: **A comparison of thermodynamic foldings with comparatively derived structures of 16S and 16S-like rRNAs**. *RNA* 1995, **1**:559–574.
- Tuerk C, MacDougall S, Gold L: **RNA pseudoknots that inhibit human immunodeficiency virus type 1 reverse transcriptase**. *Proc Natl Acad Sci USA* 1992, **89**(15):6988–6992.
- Chamorro A, Manko VS, Denisova TE: **New exact solution for the exterior gravitational field of a charged spinning mass**. *Phys. Rev. D* 1991, **44**(10):3147–3151.

7. **The pseudoknot structure of the glmS ribozyme pseudoknot P1.1**  
[<http://www.ekevanbatenburg.nl/PKBASE/PKB00276.HTM>]
8. Lyngsø RB, Pedersen CNS: **RNA pseudoknot prediction in energy-based models.** *J Comput Biol* 2000, **7**(3–4):409–427.
9. Smith TF, Waterman MS: **RNA secondary structure: A complete mathematical analysis.** *Math Biol* 1978, **42**:257–266.
10. Waterman MS, Smith TF: **Rapid dynamic programming methods for RNA secondary structure.** *Adv Appl Math* 1986, **7**(4):455–464.
11. Zuker M, Stiegler P: **Optimal computer folding of large RNA sequences using thermodynamics and auxiliary information.** *Nucl Acids Res* 1981, **9**:133–148.
12. Nussinov B, Jacobson AB: **Fast algorithm for predicting the secondary structure of single-stranded RNA.** *Proc Natl Acad Sci USA* 1980, **77**(11):6309–6313.
13. Fresco JR, Alberts BM, Doty P: **Some molecular details of the secondary structure of ribonucleic acid.** *Nature* 1960, **188**:98–101.
14. Jun IT, Uhlenbeck OC, Levine MD: **Estimation of Secondary Structure in Ribonucleic Acids.** *Nature* 1971, **230**(5293):362–367.
15. Delisi C, Crothers DM: **Prediction of RNA secondary structure.** *Proc Natl Acad Sci USA* 1971, **68**(11):2682–2685.
16. Rivas E, Eddy SR: **A dynamic programming algorithm for RNA structure prediction including pseudoknots.** *J Mol Biol* 1999, **285**(5):2053–2068.
17. Dirks RM, Lin M, Winfree E, Pierce NA: **Paradigms for computational nucleic acid design.** *Nucleic Acids Res* 2004, **32**(4):1392–1403.
18. Reeder J, Giegerich R: **Design, implementation and evaluation of a practical pseudoknot folding algorithm based on thermodynamics.** *BMC Bioinformatics* 2004, **5**(104):2053–2068.
19. Ren J, Rastegari B, Condon A, Hoos H: **Hotknots: Heuristic prediction of RNA secondary structures including pseudoknots.** *RNA* 2005, **15**:1494–1504.
20. Huang FWD, Peng WWJ, Reidys CM: **Folding 3-noncrossing RNA pseudoknot structures.** *J. Comp. Biol.* 2009, **16**(11):1549–75.
21. Borer PN, Dengler B, Tinoco JI, Uhlenbeck OC: **Stability of ribonucleic acid doublestranded helices.** *J Mol Biol* 1974, **86**(4):843–853.
22. Papanicolaou C, Gouy M, Ninio J: **An energy model that predicts the correct folding of both the tRNA and the 5S RNA molecules.** *Nucleic Acids Res* 1984, **12**:31–44.
23. Turner DH, Sugimoto N, Freier SM: **RNA structure prediction.** *Ann Rev Biophys Biophys Chem* 1988, **17**:167–192.
24. Walter AE, Turner DH, Kim J, Lyttle MH, Muller P, Mathews DH, Zuker M: **Coaxial stacking of helices enhances binding of oligoribonucleotides and improves predictions of RNA folding.** *Proc Natl Acad Sci USA* 1994, **91**(20):9218–9222.
25. Xia T, SantaLucia JJ, Burkard ME, Kierzek R, Schroeder SJ, Jiao X, Cox C, Turner DH: **Thermodynamic parameters for an expanded nearest-neighbor model for formation of RNA duplexes with Watson-Crick base pairs.** *Biochemistry* 1998, **37**(42):14719–13735.
26. Waterman MS: **Combinatorics of RNA hairpins and cloverleaves.** *Stud Appl Math* 1979, **60**:91–96.
27. D Kleitman BR: **The number of finite topologies.** *Proc Amer Math Soc* 1970, **25**:276–282.
28. Jin EY, Qin J, Reidys CM: **Combinatorics of RNA structures with pseudoknots.** *Bull Math Biol* 2008, **70**:45–67.
29. Jin EY, Reidys CM: **Combinatorial Design of Pseudoknot RNA.** *Adv Appl Math* 2009, **42**(2):135–151.
30. Chen WYC, Han HSW, Reidys CM: **Random k-noncrossing RNA Structures.** *Proc Natl Acad Sci USA* 2009, **106**(52):22061–22066.
31. Stadler PF: **RNA Structures with Pseudo-Knots.** *Bull Math Biol* 1999, **61**:437–467.
32. Ma G, Reidys CM: **Canonical RNA Pseudoknot Structures.** *J Comput Biol* 2008, **15**(10):1257–1273.
33. Huang FWD, Reidys CM: **Statistics of canonical RNA pseudoknot structures.** *J Theor Biol* 2008, **253**(3):570–578.
34. Reidys CM, Stadler PF, Schuster P: **Generic properties of combinatory maps: neutral networks of RNA secondary structures.** *Bull Math Biol* 1997, **59**(2):339–397.
35. Reidys CM: **Local connectivity of neutral networks.** *Bull Math Biol* 2008, **71**(2):265–290.
36. Hofacker I, Fontana W, Stadler P, Bonhoeffer L, Tacker M, Schuster P: **Fast folding and comparison of RNA secondary structures.** *Chem Month* 1994, **125**(2):167–188.

RNA structure	length	trials	total time	success rate
TPK-70.28 [43]	40	100	4m 57.81s	100%
Ec_PK2 [44]	59	100	5m 33.28s	100%
PMWaV-2 [45]	62	100	1m 7.12s	100%
tRNA	76	100	5m 2.49s	100%

Table 1: Inverse folding times for 100 executions of `Inv` for various RNA pseudoknot structures. In all cases all trials generated successfully sequences of the respective neutral networks.

37. Andronescu M, Fejes AP, Hutter F, Hoos HH, A C: **A New Algorithm for RNA Secondary Structure Design.** *J Mol Biol* 2004, **336**(2):607–624.
38. Busch A, Backofen R: **INFO-RNA—a fast approach to inverse RNA folding.** *Bioinformatics* 2006, **22**(15):1823–1831.
39. **3'UTR pseudoknot of bovine coronavirus** [<http://www.ekevanbatenburg.nl/PKBASE/PKB00256.HTML>].
40. Jin EY, Reidys CM: **Central and local limit theorems for RNA structures.** *J Theor Biol* 2008, **253**(3):547–559.
41. **Pseudoknot PKI of the internal ribosomal entry site (IRES) region** [<http://www.ekevanbatenburg.nl/PKBASE/PKB00221.HTML>].
42. **PseudoBase** [<http://www.ekevanbatenburg.nl/PKBASE/PKBGETCLS.HTML>].
43. **The pseudoknot of SELEX-isolated inhibitor (ligand 70.28) of HIV-1 reverse transcriptase** [<http://www.ekevanbatenburg.nl/PKBASE/PKB00066.HTML>].
44. **Pseudoknot PK2 of E.coli tmRNA** [<http://www.ekevanbatenburg.nl/PKBASE/PKB00050.HTML>].
45. **Pineapple mealybug wilt associated virus - 2** [<http://www.ekevanbatenburg.nl/PKBASE/PKB00270.HTML>].

## 8 Tables

### 8.1 Table 1